The FASEB Journal express article 10.1096/fj.04-1925fje. Published online September 27, 2004.

Differentiation of human melanoma cells induced by cyanidin-3-*O*-β-glucopyranoside

Annalucia Serafino,* Paola Sinibaldi Vallebona,[†] Giuseppe Lazzarino,[‡] Barbara Tavazzi,[§] Guido Rasi,* Pasquale Pierimarchi,* Federica Andreola,* Gabriella Moroni,[†] Giacomo Galvano,[‖] Fabio Galvano,[¶] and Enrico Garaci [†]

*Institute of Neurobiology and Molecular Medicine, National Research Council, Rome; [†]Department of Experimental Medicine and Biochemical Science, University of Rome "Tor Vergata," Rome; [‡]Department of Chemical Science, Laboratory of Biochemistry, University of Catania, Catania; [§]Institute of Biochemistry and Clinical Biochemistry, Catholic University of Rome "Sacro Cuore," Rome; [‖]Department of Agronomical, Agrochemical and Animal Production Science, University of Catania, Catania; and [¶]Department of Agro-forestry and Environmental Science, University of Reggio Calabria, Reggio Calabria, Italy

Corresponding author**:** Annalucia Serafino, C.N.R., Istituto di Neurobiologia e Medicina Molecolare, Via Fosso del Cavaliere 100, 00133 Rome, Italy. E-mail: annalucia.serafino@ims.rm.cnr.it

ABSTRACT

Great attention has been recently given to a flavonoid of the anthocyanin class, cyanidin-3-*O*-β-glucopyranoside (C-3-G), which is widely spread throughout the plant kingdom, and is present in both fruits and vegetables of human diets. In this study, we investigated the effect of C-3-G on proliferation and differentiation of human melanoma cells. Both morphological and functional parameters were evaluated, using electron and confocal microscopy, cytofluorometric analysis, HPLC assay, Western blot analysis, and enzymatic assay, as appropriate. A treatment with a single dose of C-3-G decreased cell proliferation without affecting cell viability and without inducing apoptosis or necrosis. The mitotic index and cell percentage in S phase were significantly lower in C-3-G treated cells compared with untreated control. C-3-G treatment induced, in a dose- and time-dependent manner, melanoma cell differentiation characterized by a strong increase in dendrite outgrowth accompanied with a remodeling of the microtubular network, a dramatic increase of focal adhesion and an increased expression of "brain specific" cytoskeletal components such as NF-160 and NF-200 neurofilament proteins. C-3-G treatment also induced increase of cAMP levels and up-regulation of tyrosinase expression and activity resulting in an enhanced melanin synthesis and melanosome maturation. Up-regulation of the melanoma differentiation antigen Melan-A/MART-1 in treated cells respect to the untreated control was also recorded. Data obtained provide evidence that a single treatment with C-3-G is able to revert the human melanoma cells from the proliferating to the differentiated state. We conclude that C-3-G is a very promising molecule to include in the strategies for treatment of melanoma; also because of its nutritional relevance.

Key words: anthocyanin • melanoma differentiation • electron microscopy • confocal microscopy

The incidence of melanoma is estimated to be growing at the second fastest rate among all cancers in the United States (1). Several studies have been carried out in the last years to develop more efficient and less toxic anticancer drugs for melanoma prevention and therapy. Melanocytes are epidermal cells derived from the neural crest. During embryonic development, melanocyte precursors migrate to the basal layer of the epidermis where they differentiate and acquire the ability to synthesize melanin pigment (2, 3). The differentiated state is characterized by dendrite outgrowth that ensures melanin distribution within the skin. The dendritic phenotype is also a morphological feature acquired by melanoma cells after differentiation induced by several compounds (4–6). The progression of the melanocyte to malignant melanoma involves sequential steps including benign nevocellular nevus, preneoplastic dysplastic nevus, primary melanoma, and metastatic melanoma (7–9). As in the case of all other tumors, the progression to malignant melanoma is characterized by the loss of cellular differentiation and by increased proliferation ability. In this context, it appears extremely attractive to achieve tumor reversion using differentiation inducing compounds in antitumor therapy. Recent experimental approaches have used agent(s) able to modify tumor growth by inducing terminal differentiation, a process termed "differentiation therapy" (10).

Numerous drugs derive their antitumoral activity from the ability to induce apoptosis or differentiation. Among them great attention has been given in the last decade to several natural compounds with established antioxidant activity, such as polyphenols (resveratrol; ref 11) and flavonoids (quercetin; ref 12). These substances appear very promising for the prevention of various diseases because of their consumption within the diet, and several studies have not only pointed out the antioxidant potency of resveratrol or quercetin (13) but also their anticancer efficacy in various experimental models (12, 14).

Recently, studies have also focused on determining the pharmacological profile of a flavonoid of the anthocyanin class, cyanidin-3-*O*-β-glucopyranoside (C-3-G), which is widely spread throughout the plant kingdom and is present in both fruits and vegetables of human diets (15, 16). One of the most reach dietary source of C-3-G is represented by pigmented orange (blood orange) typically growing in Sicily, Italy (17) as well as in Florida (18). In addition, C-3-G was found in its intact glycosylated form in both plasma and urine in humans and rats after oral intake of fruits (19, 20). Besides showing a remarkable ability to reduce oxidative damage mediated by reactive oxygen species (ROS), even more effectively than other natural antioxidants (21, 22), C-3-G seems to be able to induce various modifications in different tumor cell lines and in particular in human colon carcinoma cells in vitro (23), as well as in rat colorectal cancer in vivo (24). It has also been recently reported that C-3-G induces differentiation of HL-60 promyelocytic cells into macrophage-like cells and granulocytes (25).

Given this body of evidence, it appears rational to explore the possibility to include C-3-G among the tools for the treatment of melanoma. In this study, we describe the differentiating effect of C-3-G on TVM-A12, M14, and A-375 human melanoma cell lines. Because the effects were similar in all cell lines, we focused on TVM-A12 cells and provide evidence concerning the influence of this compound on cell proliferation, cell morphology, cytoskeletal organization, and melanin synthesis.

MATERIALS AND METHODS

Cell culture

The human melanoma cell line TVM-A12 was established in our laboratory from a melanoma metastatic lesion (26). The human melanoma cell lines M14 and A-375 were purchased from American Type Culture Collection (ATCC). Primary culture of human melanocytes from neonatal preputial was kindly provided by Dr. M. Picardo (S. Gallicano Dermatological Institute, Rome, Italy). All melanoma cells were grown in RPMI 1640 medium (Hyclone Labs Inc., Logan, UT) supplemented with 10% (v/v) heat-inactivated fetal calf serum (FCS) (Hyclone), L-glutamine (2 mM), penicillin (100 IU/ml), and streptomycin (100 mg/ml) at 37°C in a humidified 5% CO_2 atmosphere. Normal melanocytes were cultured in Medium 154 (Cascade Biologicals, Portland, OR) supplemented with 1% human melanocytes growth supplement (HMGS; Cascade Biologicals). All cells were passaged serially twice weekly after detachment from culture flasks with 0.05% trypsin and 0.02% EDTA solution in PBS (Hyclone). TVM-A12 cells were used between passages 80 and 110, M14 and A-375 between passages 30 and 40, and human melanocytes between passages 3 and 6.

Chemicals

C-3-G was purchased from Polyphenols AS Laboratories (Hanabryggene Technology Centre, Sandnes, Norway). Retinoic acid (RA) was obtained from Sigma-Aldrich (St. Louis, MO). Ultrapure standards for high performance liquid chromatographic (HPLC) analyses were supplied by Boheringer (Ingelheim GmbH, Germany) and tetrabutylammonium hydroxide, used as the ion-pairing reagent for the HPLC analysis of cAMP compound, was purchased as a 55% aqueous solution from Nova Chimica (Cinisello Balsamo, Milan, Italy).

Cell treatments

Exponentially growing human melanoma cells were seeded at density of 5 x 10^4/ml (25 cm^2 flasks) and incubated for 24 h before treatments. At the end of this period, cells were treated with a single dose of 5 or 10 μM C-3-G and maintained in culture for a different period of time. RA (5 or 10 μM), a well-known melanoma-differentiating agent (27, 28), was used as positive control. C-3-G was dissolved in DMSO at a final concentration of DMSO not higher than 0.001% in all experiments. RA was dissolved in 70% ethanol to obtain a 5 mM stock solution. Concentrations were selected on the basis of the lowest effective doses find in a dose-response experiment (not shown). For any microscopic analysis, cells were grown on coverslip.

Viability assay and mitotic index evaluation

For determination of C-3-G cytotoxicity on TVM-A12, cells were seeded at a density of 5 x 10^4 per well onto 24-well cell culture plates and allowed to adhere for 24 h. Thereafter, treatment compounds were added to culture medium and cells were allowed to grow for a time ranging from 3 h to 6 days. Controls consisted of cells cultured in DMSO containing medium. Cell viability was determined at indicated times, based on the Trypan blue dye exclusion method. To evaluate the mitotic index, cell nuclei were stained with 2 μg/ml propidium iodide (PI) in the presence of 0.1 mg/ml RNAase (Sigma-Aldrich Co., St. Louis, MO) and mitotic cells were counted. A minimum of 1000 cells per sample were observed using a confocal microscopy.

Flow-cytometric cell cycle analysis

The cell cycle was analyzed by measuring bromodeoxyuridine (BrdU) incorporation and total amount of DNA by PI staining. To measure BrdU incorporation, 1,000,000 of treated and untreated TVM-A12 cells were incubated with 30 μg/ml BrdU (Sigma-Aldrich) in serum-free media for 30 min. Cells were washed twice in cold PBS, harvested from flasks by a rubber policeman, and resuspended in 4 ml of ice-cold PBS. While vortexing, 6 ml of ice-cold 100% ethyl alcohol was slowly added to the cells and samples were fixed overnight at -20°C. Cells were centrifuged at 100 *g* for 5 min and resuspended in pepsin solution (0.04% pepsin in 0.1% HCl) for 1 h at 37°C with gentle shaking. Cells were pelleted at 100 *g* for 5 min, resuspended in 3 ml of 2 N HCl, and then incubated for 30 min at 37°C. To this solution, 6 ml of 0.1 M sodium borate was added, vortexed for 20 s, and then recentrifuged. Cells were washed once and brought to a final volume of 200 μl with wash buffer (0.5% BSA and 0.5% Tween 20 in PBS). Fluorescein isothiocyanate (FITC)-conjugated anti-BrdU antibody (Becton-Dickinson) was added in a 1:20 dilution, and the mixture was allowed to incubate in the dark for 60 min at room temperature. Samples were then washed once with wash buffer and resuspended in 1 ml of 10 μg/ml PI plus 0.1 mg/ml RNAase (Sigma-Aldrich) in wash buffer for 30 min at 37°C. The sample was passed through a 21G needle and transferred to a Falcon 35-2052 vial and read by FACS-Scan (Becton-Dickinson). The experiment was repeated three times, and the mean values were plotted.

Optical microscopy

Treated and untreated TVM-A12, M14, and A-375 human melanoma cells and normal melanocytes were stained with Wright Giemsa and observed by phase-contrast microscopy after 5 days of culture.

Scanning electron microscopy

Treated and untreated TVM-A12 cells were fixed with 2.5% glutharaldehyde in 0.1 M Millonig's phosphate buffer (MPB; to obtain 100 ml: 32 ml 2 M sodium-dihydrogen-orthophosphate, 14 ml 2 M di-sodium-hydrogen-orthophosphate, 50 ml DDW, pH 7.4 were mixed) at 4°C for 1 h. After being washed in MPB, cells were postfixed with 1% OsO_4 in the same buffer for 1 h at 4°C and dehydrated using increasing acetone concentrations. The specimens were critical-point dried using liquid CO_2 and sputter coated with gold before examination on a Stereoscan 240 scanning electron microscope (Cambridge Instr., Cambridge, UK).

Immunofluorescence labeling and confocal laser scanning microscopy

Treated and untreated TVM-A12 cells were fixed with 4% paraformaldehyde for 10 min and permeabilized with 0.2% Triton-X 100 in PBS for 5 min. Samples were subjected to indirect immunofluorescence staining using the following primary antibodies: *1*) mAb to human vinculin (Sigma-Aldrich); *2*) mAbs to neurofilament proteins NF-68 kDa, NF-160 kDa, and NF-200 kDa (Sigma-Aldrich); and *3*) rabbit polyclonal antibody raised against chicken tubulin (Sigma-Aldrich). Primary antibody detection was obtained by reaction with fluorescein(FITC)-conjugated IgG (Sigma-Aldrich). Cell nuclei were stained with 2 μg/ml PI (Sigma-Aldrich) in the presence of 0.1 mg/ml RNAase (Sigma-Aldrich). For evaluation of neurofilament proteins

expression, at least 500 cells per sample, in three different experiments, were examined for immunofluorescence. As control, neurofilament protein expression was also tested in normal human melanocytes processed and subjected to indirect immunofluorescence staining for NF-160 kDa and NF-200 kDa as described previously.

Fluorescently labeled samples were imaged by a confocal LEICA TCS 4D microscope (Leica, Heidelberg, Germany) equipped with an argon/kripton laser. Confocal sections were taken at 0.5-1 μm intervals. The excitation and emission wavelengths were 488 and 510 nm, respectively, for FITC-labeling, and 568 and 590 nm, respectively, for PI.

Transmission electron microscopy and quantitative image analysis

Treated and untreated TVM-A12 cells were fixed with 2.5% glutheraldheide in 0.1 M MPB containing 2% sucrose and then postfixed with 1% OsO_4 in the same buffer. Samples were then scrapped out from plates, dehydrated in ascending ethanol concentrations, and embedded in Spurr epoxy resin (Agar Scientific LTD, Stansted, Essex, UK). Ultrathin sections were stained with uranyl acetate and lead citrate and observed under a Philips CM12 transmission electron microscope operating at 80 kV. For quantitative analysis of melanosome area density and degree of maturation, a minimum of 10 cells for each experimental condition were randomly selected. The total number of melanosomes in each group was obtained by counting trice the number of organelles in middle section of each cell, and then the values were averaged. Classification of melanosome maturation stages was performed within the same cells used to obtain the relative number of melanosomes. To avoid classification errors, stages I and II melanosomes were considered in the same group, as reported by others (29). The melanosomal index in each maturation stage was calculated by dividing the number of each type of melanosome by the total number of melanosomes counted in each cell. The melanosome area density (defined as the percentage of total melanosomal area to total cytoplasm area in each cell) was obtained by quantitative image analysis using the ImageJ processing program downloaded from the National Institutes of Health (NIH) web site. The area corresponding to the melanosomes and the cell cytoplasm area, used as a reference space, were manually delimited.

HPLC assay of cAMP on cell extracts

At the end of each incubation period, cells were gently scraped, centrifuged, and then washed threefold with 10 mM glucose-supplemented phosphate buffered saline (PBS-glucose). After the third wash, packed cells were deproteinized by adding ice-cold 1.2 M $HClO_4$ (1:2; w:v) and centrifuged at 20,690 *g* for 10 min at 4°C. Pellets were saved, and supernatants were neutralized by adding 5 M K_2CO_3 in the cold and were centrifuged again at 20,690 *g* (10 min at 4°C). Supernatants were extracted by vigorous agitation with a double volume (2:1; v:v) of HPLC-grade CH_3Cl and centrifuged as above. The upper aqueous phases (containing water-soluble low-molecular weight compounds) were collected, subjected to chloroform washings for one more time (this procedure allowed the removal of any lipid soluble compound from the buffered cell extracts), and then saved at -80°C. Cell pellets were vortexed with 2 ml chloroform, centrifuged again to eliminate chloroform, dried with a gentle stream of nitrogen, and resuspended with 100 μl of 10 mM KH_2PO_4, pH 7.40. After 24 h at 4°C, pellets were centrifuged and the supernatants were collected and added to the corresponding aqueous cell extracts and stored at –80°C. Aliquots of each extract were filtered through a 0.45 μm HV-Millipore filter and assayed by ion-pairing HPLC for detection of cAMP and adenine nucleotide derivatives according to

modifications of already established methods (30, 31). Separation was carried out on 200 µl using a Kromasil 250 × 4.6 mm, 5 µm particle size column, provided with its own guard column (Eka Chemicals AB, Bohus, Sweden). The HPLC apparatus consisted of a SpectraSystem P2000 pump (ThermoQuest, Rodano, Milan, Italy) connected to a highly sensitive UV6000 LP diode array spectrophotometric detector (ThermoQuest, Rodano, Milan, Italy), equipped with a 5 cm light path flow cell and set up between 200 and 300 nm for data acquisition. A step gradient from buffer A (10 mM tetrabutylammonium hydroxide, 10 mM KH_2PO_4, 0.125% methanol, pH 7.00) to buffer B (2.8 mM tetrabutylammonium hydroxide, 100 mM KH_2PO_4, 30% methanol, pH 5.50) was formed as follows: 10 min 100% buffer A; 3 min at up to 80% buffer A; 10 min at up to 70% buffer A; 12 min at up to 55% buffer A; 11 min at up to 40% buffer A; 9 min at up to 35% buffer A; 10 min at up to 25% buffer A; 15 min 0% buffer A; 5 min 0% buffer A. Flow rate of 1.2 ml/min and constant column temperature of 23°C were also used. Peaks of chromatographic runs of cell extracts were identified by comparing retention times and absorption spectra with those of freshly prepared ultra-pure standard mixtures. Concentrations of the diverse compounds were calculated by comparing peak areas with those of standard mixtures with known concentrations, at the wavelengths corresponding to the maximum of absorption of each substance. Acquisition and analysis of data were performed by a PC using the ChromQuest® software package provided by the HPLC manufacturer.

Western blot analysis

For tyrosinase and Melan-A/MART-1 antigen immunoblot detection, cells were lysed in phosphate buffer, pH 6.8, containing 1% Triton-X 100, 100 IU/ml aprotinin, and 1 mM PMSF. The solubilized proteins (40γ) were loaded on to 12% SDS-polyacrylamide gels and transferred on to nitrocellulose (Biorad Labs., Hercules). The membranes were saturated with 5% powdered milk in PBS containing 0.05% Tween (PBST), and tyrosinase or Melan-A/MART-1 as detected with the mouse monoclonal antibodies anti-tyrosine hydroxylase (Sigma-Aldrich: working dilution 1:1000 in the saturation buffer) or Melan-A A103 (Santa Cruz Biotechnology, Santa Cruz, CA: working dilution 1:2000), respectively, followed by a secondary peroxidase-conjugated anti-mouse antibody (Amersham Biosciences, Uppsala, Sweden) at a 1:10,000 dilution. After the antibody incubation, three 10 min washes with PBST were performed. The blots were developed using the Super Signal System from Pierce (Rockford, IL).

Tyrosinase activity determination

Tyrosinase activity was estimated by measuring the rate of oxidation of L-DOPA (32). Cellular extract was obtained as described for Western Blot analysis. The tyrosinase substrate L-DOPA (2 mg/ml; Sigma-Aldrich) was prepared in the same lysis buffer (without Triton-X 100). Forty microliters of each extract were put in a 96-well plate, and the enzymatic assay was started by adding 100 µl of L-DOPA solution at 37°C. Control wells contained 40 µl of lysis buffer. Absorbance at 570 nm was read every 10 min for at least 1 h at 37°C using the microplate reader Multiscan Ex (Labsystems, Farnborough, Hampshire, UK). The blank was removed from each absorbance value, and the final activity was corrected by the total amount of protein content for each experimental condition.

Statistical analysis

For statistical analysis, Student's *t* test was used. For each variable, at least three independent experiments were carried out. Data are given as the means ± SD.

RESULTS

Effect of C-3-G treatment on cell viability and proliferation

C-3-G affected TVM-A12 cell viability to lower extent respect then RA, as determined by the Trypan blue exclusion method (Fig. 1*A*). Cell nuclei labeled using PI and observed by confocal microscopy did not show any apoptotic or necrotic figures in C-3-G treated cells, confirming the lower toxicity of this compound compared with RA, which conversely induced apoptosis in a dose- and time-dependent fashion (not shown). Furthermore, C-3-G treatment caused a decrease of cell proliferation in a similar but more efficient manner than RA. In fact, the mitotic index was significantly lower ($P<0.0001$) in C-3-G treated cells compared with untreated control at any time but particularly evident within 24 h, where it is also significantly lower compared with RA (Fig. 1*B*). It should be noted that untreated cells were in confluent monolayer after 6 days of culture, and this may explain the low mitotic index recorded in this sample. To confirm the antiproliferative effect induced by C-3-G, we also performed cytofluorometric analysis of cell cycle by measuring BrdU incorporation and total amount of DNA by PI staining to evaluate changes in the S phase cell population within 24 h of treatment. Time was chosen on the information obtained by mitotic index data (Fig. 1*B*). Analysis of BrdU incorporation in C-3-G or RA treated cells indicated, already after 2 h of treatment and for each other time point examined, an evident decrease of cell percentage in S phase compared with untreated control (Fig. 1*C*). This antiproliferative effect was more evident for C-3-G respect to RA, and it is not due to cytotoxicity of treatment, as shown by viability assay at 3 h and 1 day of culture (Fig. 1*A*). These data also indicated that changes in cell cycle distribution occurred within 8 h of treatment, suggesting the involvement of very early event(s).

Morphological differentiation induced by C-3-G treatment

We analyzed the effect of C-3-G treatment on cell morphology and compared it to the effect of RA. RA affects a wide variety of biological processes, and it is known to induce dendrite outgrowth in melanocyte and melanoma cells (26, 27). By phase-contrast microscopy, (Fig. 2), we observed that a single treatment of C-3-G, similarly to RA, strongly stimulated cell dendricity, which is a morphological feature of differentiated melanocytes (Fig. 2*A* and *B*) and the first observable parameter of melanoma cell differentiation. After both C-3-G and RA treatments, the dendritic phenotype was acquired not only by TVM-A12 cells (Fig. 2*C–E*) but also by other two human melanoma cell lines: A-375 (Fig. 2*F–H*) and M14 cells (Fig. 2*I–K*); this observation confirmed that the stimulation of cell dendricity was not a cell line specific effect.

Scanning electron microscopy observation (Fig. 3*A–C*) showed that both C-3-G and RA treated cells acquired the differentiated melanocytic phenotype, including dramatic dendrite extensions (detailed in Fig. 3*B* and *C*) as compared with untreated cells that have a spindle-shaped morphology (Fig. 3*A*). These differentiating features were even more evident, increasing exposure time and drug concentration (not shown).

Effect of C-3-G treatment on cytoskeleton components

We compared the organization of the microtubular network in C-3-G or RA treated and untreated cells by staining with rabbit polyclonal antibody raised against tubulin to investigate whether the dendritic phenotype acquired by TVM-A12 cells after treatment with both C-3-G and RA was accompanied by a redistribution of cytoskeleton components. As shown in Fig. 3*D–F*, C-3-G treatment, similarly to RA, induced a remodeling of the microtubular network in the cytosol: the microtubular structures disappeared from the perinuclear region and appeared in the cell periphery, and the growing dendrites contained well-organized microtubules (arrows in Fig. 3*E* and *F*), suggesting the involvement of a tubulin polymerization-dependent process in dendrite outgrowth. The reorganization of microtubular network was more evident, increasing exposure time and drug concentration (not shown).

C-3-G treatment, similarly to but more efficiently than RA, also modified the distribution of vinculin (Fig. 3*G–I*), a cytoskeletal component of substratum adhesion plaques, inducing a dramatic increase of focal adhesions, localized below and at the borders of cells and along the growing dendrites, particularly evident after 24 h treatment (Fig. 3*H* and *I*).

Finally, to investigate whether the acquisition of neuron-like phenotype by both C-3-G and RA treated melanoma cells was accompanied with the expression of "brain specific" cytoskeletal components such as neurofilament proteins (NFPs), we tested treated cells and untreated control for the presence of the three isoforms of NFPs, namely NF-68 kDa, NF-160 kDa, and NF-200 kDa by indirect immunofluorescence technique. A significant increase ($P<0.001$), compared with the control, in the percentage of positive cells was recorded for the NF-200 kDa and, at a higher level, for the NF-160 kDa subunits, in both C-3-G and RA treated cells, as shown in Fig. 4*M*, while no immunoreaction was observed for the NF-68 kDa subunit in both treated and untreated cells. In detail, the percentage of positive cells for the NF-200 kDa subunit, which in the untreated control was ~14%, increased to ~18% after 5 days RA treatment and to ~40% after 5 days C-3-G-treatment. A greater increase in the percentage of positive cells was observed for the NF-160 kDa subunit, which increased from 5% in control to 48% after 5 days RA treatment and to 73% after 5 days C-3-G-treatment. Furthermore, for both treatments we observed a similar pattern of intracellular distribution of the neurofilament network (Fig. 4*A–L*); while the NF-200 kDa subunit appeared organized as filamentous structures and distributed throughout the dendritic extensions (Fig. 4*E*, *F*, *I*, and *J*), the NF-160 kDa subunit exhibited a granular pattern mainly located in the perinuclear region and a mesh-like pattern distributed in the outgrowing dendrites (Fig. 4*G*, *H*, *K*, and *L*). To demonstrate that an increase in the expression of "brain specific" cytoskeletal components such as neurofilament proteins was connected with a differentiated melanocitic phenotype, we also tested, by indirect immunofluorescence technique, the expression of NF-160 kDa and NF-200 kDa in primary culture of normal human melanocytes (Fig. 4*N–Q*). About 100% of melanocytes expressed both NF-160 kDa and NF-200 kDa, as shown in Fig. 4*M*; the intracellular distribution of NF-160 kDa and NF-200 kDa in melanocytes showed a pattern similar to that observed in C-3-G or RA treated TVM-A12 human melanoma cells described previously.

Effect of C-3-G treatment on melanin synthesis

Phase-contrast microscopy observation showed that C-3-G induced, similarly to RA, a dramatic increase in melanin content in TVM-A12 cells (Fig. 5*A–C*). To better investigate the possible

effect of C-3-G treatment on melanin formation and melanosome maturation, we first analyzed the relative melanosome number and maturation stages, in treated and untreated cells, by transmission electron microscopy (Fig. 5*D–J*) and quantitative image analysis (Fig. 6). In untreated control, melanosomes were scarce, small and randomly distributed throughout the cytoplasm (Fig. 5*D* and *G*). Conversely, in RA and, at higher extent, in C-3-G treated cells, melanosomes were increased in number and size (Fig. 5*E*, *F*, *H*, and *I*), as also confirmed by quantitative image analysis of the melanosome area density (Fig. 6*A*) and of the number of melanosomes per cell (Fig. 6*B*), in each experimental condition. Furthermore, both the ultrastructural analysis (Fig. 5*G–J*) and the estimation of the relative portions of melanosomes in the different maturation stages (Fig. 6*C*), showed that in treated cells the late stages (III and IV stages) of the melanosomes maturation process were more represented in respect to the early stages (premelanosomes: I and II stages), compared with the untreated control. Moreover, in C-3-G treated cells, huge complexes resulting from the aggregation of multiple melanosomes were more often observed (Fig. 5*J*). To study the molecular events leading to the increase of melanin synthesis and melanosomes maturation induced by C-3-G, we analyzed, in each experimental condition, the intracellular levels of cyclic AMP (cAMP), a key messenger in the regulation of melanogenesis (33), and both expression and activity of tyrosinase, the specific enzyme required for proper melanin production. A time-dependent increase in the intracellular cAMP content was recorded for RA and, at higher extent, for C-3-G treatment, with respect to the untreated control, by HPLC analysis (Fig. 7*A*). C-3-G treatment also induced an up-regulation of tyrosinase expression in TVM-A12 cells (Fig. 7*Ba*) as well as a stimulation of ~2.5 fold of tyrosinase activity (Fig. 7*C*), as revealed by Western blot analysis and enzymatic assay, respectively. All these molecular events strongly support the evidence of melanoma differentiation, since pigmentation is a marker of melanocytes differentiation.

Effect of C-3-G treatment on expression of Melan-A/MART-1

Finally, to further characterize the differentiating effect induced by C-3-G, we analyzed the expression of an additional molecule, beside the tyrosinase, involved in melanoma differentiation, the extensively studied Melan-A/MART-1 antigen. Melan-A/MART-1 is a melanocytic differentiation antigen, expressed in melanocytes and melanoma cells (34, 35), which is recognized by cytotoxic T-lymphocytes (36) and for this reason is of great interest for clinicians as a potential immunotherapeutic target and for pathologists as a possible diagnostic marker. As reported in Fig. 7*Bb*, Western blot analysis of Melan-A/MART-1 expression showed, after 5 days of culture, in both samples treated with C-3-G or RA an up-regulation of this antigen compared with the untreated control. This effect was much higher in C-3-G treated cells than in RA treated culture.

DISCUSSION

During the last years, great attention has been given to a variety of dietary substances, such as resveratrol, β-carotene, vitamins A, C, and D, for treatment and prevention of skin cancer (37). It has been suggested that these compounds, due to their antioxidant properties, may support the endogenous antioxidant system of the skin that scavenges reactive oxygen species (ROS) and combat the ultraviolet light induced oxidative skin damage. Because it is known that ROS play key roles in the regulation of proliferation and differentiation of many cell type and that altered redox control may be involved in melanoma genesis (38, 39), dietary factors with antioxidant properties have been proposed for prevention and treatment of many cancers and in particular of

melanoma (37, 40). The flavonoid of the anthocyanin class, C-3-G, is widely spread in the plant kingdom, in both fruits and vegetables (15, 16) and possesses remarkable ability to reduce oxidative damages mediated by ROS (21, 22). Like other flavonoids, anthocyanins can act as antitumor agents in vitro and in vivo (41, 42), and in particular cyanidin has been reported to inhibit the cellular growth of human colon carcinoma cells in vitro and in rat colorectal cancer in vivo (23, 24).

In the present work, we provide evidence that a single treatment with C-3-G is able to induce differentiation in TVM-A12 human melanoma cell line and reverts the cells from the proliferating to the differentiated state. The differentiation pathway, characterized by growth inhibition, reorganization of microtubular network, and dendrite outgrowth, is similar to that observed in cells treated with RA, which has been reported to modulate cell growth and differentiation and found to suppress tumor cell invasion in vitro and appearance of metastasis in vivo (26, 43, 44). The dendritic phenotype was also acquired, after C-3-G treatment, by other two human melanoma cell lines, A-375 and M14 cells, thus confirming that the induction of cell dendricity was not a cell line specific effect.

In addition, the absence of apoptosis or necrosis in C-3-G treated cells at the used concentrations indicates that this compound posseses a very low toxicity when compared with RA. The acquisition of a neuron-like phenotype in both C-3-G and RA treated cells is accompanied by a strong increase, much more evident for C-3-G vs. RA, in the expression of "brain specific" cytoskeletal component such as the neurofilament proteins NF-160 kDa and NF-200 kDa subunits, which are weakly expressed in untreated TVM-A12 melanoma cells. Because melanocytes are neural crest derivatives, we speculate that the observed increase in the expression of neuronal markers such as neurofilament proteins is associated with regression of tumor cells toward a less malignant and less invasive neoplastic form. Supporting this hypothesis are data indicating that various neural protein markers such as the microtubule-associated protein 2 (MAP-2), the low-affinity nerve growth factor receptor (p75NGFR) and the neural cell adhesion molecule (CD56/N-CAM) are abundantly expressed in melanocytes, in nevus cells, and in some cases in primary melanomas but are weakly or not expressed in metastatic melanomas (45, 46). Furthermore, our results concerning the expression of the neurofilament proteins NF-160 kDa and NF-200 kDa in primary culture of melanocytes, confirm the correlation between increasing in the expression of these NFPs and a more differentiated and less malignant phenotype.

The results relative to the redistribution of vinculin, a cytoskeletal component involved in cell-substratum contacts, show a transition from an intermediate state of adherence, in the untreated controls, to a strongly adherent state with increased focal adhesion. Since it has been reported that the strong adhesive state is characteristic of a differentiated, quiescent cells (47), the dramatic increase of focal adhesions observed after C-3-G treatment supports the hypothesis of the differentiation. This finding also suggests that the C-3-G treatment might lead to a decreased motility and to an increased adhesiveness as a consequence of vinculin reorganization. Additionally, C-3-G treatment also would be expected to decrease the metastatic potential of our melanoma cells to a greater extent than RA. Tumor metastasis and invasion have been reported to be inhibited by vitamin C through decreasing the oxidative stress (48).

Concerning the mechanism underlying the antiproliferative and differentiating effect of C-3-G on melanoma cells, we can asses that the effectiveness of this compound is based on its

interaction with cells in its intact form. In fact, the differentiated phenotype has been observed exclusively using the whole molecule, while no effect has been induced by treatment with the related aglycon (data not shown). Supporting our assumption are studies demonstrating that C-3-G was found in its intact glycosylated form in both plasma and urine in humans and rats after oral intake of fruits (19, 20).

A single treatment of C-3-G also influences the melanin formation and melanosome maturation in TVM-A12 human melanoma cells, as demonstrated by transmission electron microscopy and quantitative image analysis data. The melanogenic effect of C-3-G appears to be mediated through the up-regulation of the cAMP pathway accompanied with an increase in both expression and activity of tyrosinase, the enzyme that controls the specific enzymatic pathway of melanin synthesis. cAMP-elevating agents are known to induce melanoma cell differentiation, characterized by increased melanin synthesis and dendrite outgrowth (4, 49). It has also been reported that the cAMP pathway may play a pivotal role in the regulation of the activity and/or expression of melanogenic enzymes (33). Moreover, C-3-G treatment, by influencing melanin formation and melanosome maturation, may also have a chance of decreasing the incidence of ultraviolet induced carcinogenesis. Furthermore, in C-3-G treated cells overexpression of tyrosinase is accompanied with a dramatic up-regulation of the melanocytic differentiation antigen Melan-A/MART-1. The intracellular distribution of Melan-A/MART-1 in C-3-G and RA treated cells was similar to that observed by immunofluorescence study in primary culture of normal melanocytes where this antigen is expressed in the 100% of cells (data not shown). This observation confirms the correlation between the increased expression of this antigen with a more differentiated and less malignant phenotype.

In conclusion, our results provide morphological and functional evidence that a single treatment with the anthocyanin C-3-G is able to revert human melanoma cells from the proliferating to the differentiated state. What is particularly encouraging is that C-3-G is active at concentrations corresponding to those achieved with food intake (range of μM) and without any toxicity. Although further studies will be necessary to understand the molecular mechanism underlying the differentiating effect induced by C-3-G on human melanoma cells, our results provide a new perspective in the development of novel strategies for the prevention and treatment of melanoma through consumption of C-3-G in an appropriate cancer prevention diet.

ACKNOWLEDGMENTS

The authors would like to thank Luana Mercuri, Manuela Zonfrillo, and Fabio Falcione for technical assistance and Dr. Angelo Russo, M.D., for help in critically reviewing the manuscript. This work was partially supported by “Contributo per Progetti di Ricerca anno 2003- Università Cattolica del Sacro Cuore, Roma” Grant Number 7020269; by “Funds of Provincia Regionale di Catania,” Research Contract on “Antioxidant properties of sicilian pigmented oranges”; and by Ministero della Salute: Progetto ricerca finalizzata 2002; Project title: “Sviluppo di nuove strategie di immunoterapia e terapie combinate contro i tumori" Grant Number 3AO/F5 and Progetto ricerca finalizzata 2003: Sviluppo di nuove strategie antitumorali: identificazione dei target subcellulari mediante l’applicazione di metodologie avanzate” Grant Number 4AA/F8.

REFERENCES

1. Burton, R. B. (2000) Malignant melanoma in the year 2000. *CA Cancer J. Clin.* **50,** 209–213

2. Fitzpatrick, T. D., Szabo, G., Seiji, M., and Quevedo, W. C. (1979) Biology of melanin pigmentary system. In *Dermatology in General Medicine* (Fitzpatrick T., ed) pp. 131-163, Academic Press, New York

3. Le Douarin, N. (1982) *The Neural Crest*. Cambridge University Press, Cambridge, UK

4. Buscà, R., Berlotto, C., Ortonne, J. P., and Ballotti, R. (1996) Inhibition of the phosphatidylinositol 3-kinase pathway induces B16 melanoma cell differentiation. *J. Biol. Chem.* **271,** 31824–31830

5. Kosano, H., Kayanuma, T., and Nishigori, H. (2000) Stimulation of melanogenesis in murine melanoma cells by 2-mercapto-1-(beta-4-pyridethyl) benzimidazole (MPB). *Biochem. Biophys. Acta* **1499,** 11–18

6. Pantazis, P., Chatterjee, D., Han, Z., and Wyche, J. (1999) Differentiation of human malignant melanoma cells that escape apoptosis after treatment with 9-nitrocamptothecin in vitro. *Neoplasia* **1,** 231–240

7. Houghton, A. N., Eisinger, M., Albino, A. P., Cairncross, J. G., and Old, L. J. (1982) Surface antigens of melanocytes and melanomas markers of melanocyte differentiation and melanoma subsets. *J. Exp. Med.* **56,** 1755–1766

8. Newton Bishop, J. A. (1997) Molecular pathology of melanoma. *Cancer Metastasis Rev.* **16,** 141–154

9. Holzmann, B., Brocker, E. B., Lehmann, J. M., Ruiter, D. J., Sorg, C., Riethmuller, G., and Johnson, J. P. (1987) Tumor progression in human malignant melanoma five stages defined by their antigenic phenotypes. *Int. J. Cancer* **39,** 466–471

10. Waxman, S. (2000) Differentiation therapy in acute myelogenous leukemia (non-APL). *Leukemia* **14,** 491–496

11. Cal, C., Garban, H., Jazirehi, A., Yeh, C., Mizutani, Y., and Bonavida, B. (2003) Resveratrol and cancer chemoprevention apoptosis and chemo-immunosensitizing activities. *Curr. Med. Chem. Anti-Canc. Agents* **3,** 77–93

12. Lopez-Lazaro, M., and Akiyama, M. (2002) Flavonoids as anticancer agents structure-activity relationship study. *Curr. Med. Chem. Anti-Canc. Agents* **2,** 691–714

13. Sovak, M. (2001) Grape extract resveratrol and its analogs. A Review. *J. Med. Food* **4,** 93–105

14. Savouret, J. F., and Quesne, M. (2002) Resveratrol and cancer: a review. *Biomed. Pharmacother.* **56,** 84–87

15. Wang, H., Race, E. J., and Shrikhande, A. J. (2003) Characterization of anthocyanins in grape juices by ion trap liquid chromatography-mass spectrometry. *J. Agric. Food Chem.* **51,** 1839–1844

16. Seeram, N. P., Cichewicz, R. H., Chandra, A., and Nair, M. G. (2003) Cyclooxygenase inhibitory and antioxidant compounds from crabapple fruits. *J. Agric. Food Chem.* **51,** 1948–1951

17. Amorini, A. M., Fazzina, G., Lazzarino, G., Gavazzi, B., Di Pierro, D., Santucci, R., Sinibaldi, F., Galvano, F., and Galvano, G. (2001) Activity and mechanism of the antioxidant properties of cyanidin-3-O-beta-glucopyranoside. *Free Radic. Res.* **35,** 953–966

18. Lee, H. S. (2002) Characterization of major anthocyanins and the color of red-fleshed Budd Blood orange (*Citrus sinensis*). *J. Agric. Food Chem.* **50,** 1243–1246

19. Matsumoto, H., Inaba, H., Kishi, M., Tominaga, S., Hirayama, M., and Tsuda, T. (2001) Orally administered delphinidin 3-rutinoside and cyanidin 3-rutinoside are directly absorbed in rats and humans and appear in the blood as the intact forms. *J. Agric. Food Chem.* **49,** 1546–1551

20. Tsuda, T., Horio, F., and Osawa, T. (1999) Absorption and metabolism of cyanidin 3-O-beta-D-glucoside in rats. *FEBS Lett.* **449,** 179–182

21. Ichikawa, H., Ichiyanagi, T., Xu, B., Yoshii, Y., Nakajima, M., and Konishi, T. (2001) Antioxidant activity of anthocyanin extract from purple black rice. *J. Med. Food* **4,** 211–218

22. Kahkonen, M. P., and Heinonen, M. (2003) Antioxidant activity of anthocyanins and their aglycons. *J. Agric. Food Chem.* **51,** 628–633

23. Briviba, K., Abrahamse, S. L., Pool Zobel, B. L., and Rechkemmer, G. (2001) Neurotensin- and EGF-induced metabolic activation of colon carcinoma cells is diminished by dietary flavonoid cyanidin but not by its glycosides. *Nutr. Cancer* **41,** 172–179

24. Hagiwara, A., Miyashita, K., Nakanishi, T., Sano, M., Tamano, S., Kadota, T., Koda, T., Nakamura, M., Imaida, K., Ito, N., et al. (2001) Pronounced inhibition by a natural anthocyanin purple corn color of 2-amino-1-methyl-6-phenylimidazo[4,5-b]pyridine (PhIP)-associated colorectal carcinogenesis in male F344 rats pretreated with 1-2-dimethylhydrazine. *Cancer Lett.* **171,** 17–25

25. Fimognari, C., Berti, F., Nusse, M., Cantelli-Forti, G., and Hrelia, P. (2004) Induction of apoptosis in two human leukemia cell lines as well as differentiation in human promyelocytic cells by cyanidin-3-O-beta-glucopyranoside. *Biochem. Pharmacol.* **67,** 2047–2056

26. Melino, G., Sinibaldi-Vallebona, P., D'Atri, S., Annicchiarico-Petruzzelli, M., Rasi, G., Catani, M. V., Tartaglia, R. L., Vernole, P., Spagnoli, L. G., Finazzi-Agrò, A., et al. (1993) Characterization of three melanoma cell lines (TVM-A12, TVM-A197, TVM-BO) sensivity to lysis and effect of retinoic acid. *Clin. Chem. Enzym. Comms.* **6,** 105–119

27. Demary, K., Wong, L., and Spanjaard, R. A. (2001) Effects of retinoic acid and sodium butyrate on gene expression histone acetylation and inhibition of proliferation of melanoma cells. *Cancer Lett.* **163,** 103–107

28. Niles, R. M. (2003) Vitamin A (retinoids) regulation of mouse melanoma growth and differentiation. *J. Nutr.* **133,** 282S–286S

29. Martinez-Esparza, M., Ferrer, C., Castells, M. T., Garcia-Borron, J. C., and Zuasti, A. (2001) Transforming growth factor beta1 mediates hypopigmentation of B16 mouse melanoma cells by inhibition of melanin formation and melanosome maturation. *Int. J. Biochem. Cell Biol.* **33,** 971–983

30. Lazzarino, G., Di Pierro, D., Tavazzi, B., Cerroni, L., and Giardina, B. (1991) Simultaneous separation of malondialdehyde, ascorbic acid, and adenine nucleotide derivatives from biological samples by ion-pairing high-performance liquid chromatography. *Ann. Biochem.* **197,** 191–196

31. Di Pierro, D., Tavazzi, B., Perno, C. F., Bartolini, M., Balestra, E., Caliò, R., Giardina, B., and Lazzarino, G. (1995) An ion-pairing high-performance liquid chromatographic method for the direct simultaneous determination of nucleotides, deoxynucleotides, nicotinic coenzymes, oxypurines, nucleosides, and bases in perchloric acid cell extracts. *Ann. Biochem.* **231,** 407–412

32. Takahashi, H., and Parsons, P. G. (1992) Rapid and reversible inhibition of tyrosinase activity by glucosidase inhibitors in human melanoma cells. *J. Invest. Dermatol.* **98,** 481–487

33. Buscà, R., and Ballotti, R. (2000) Cyclic AMP a key messenger in the regulation of skin pigmentation. *Pigment Cell Res.* **13,** 60–69

34. Chen, Y. T., Stockert, E., Jungbluth, A., Tsang, S., Coplan, K. A., Scanlan, M. J., and Old, L. J. (1996) Serological analysis o Melan-A (MART-1), a melanocyte-specific protein homogeneously expressed in human melanomas. *Proc. Natl. Acad. Sci. USA* **93,** 5915–5919

35. Busam, K. J., Chen, Y. T., Old, L. J., Stockert, E., Iverson, K., Coplan, K. A., Rosai, J., Barnhill, R. L., and Jungbluth, A. A. (1998) Expression of Melan-A (MART-1) in benign melanocytic nevi and primary cutaneous malignant melanoma. *Am. J. Surg. Pathol.* **22,** 976–982

36. Kirkin, A. F., Dzhandzhugazyan, K., and Zeuthen, J. (1998) Melanoma-associated antigens recognized by cytotoxic T lymphocytes. *APMIS* **106,** 665–679

37. Bialy, T. L., Rothe, M. J., and Grant-Kels, J. M. (2002) Dietary factors in the prevention and treatment of nonmelanoma skin cancer and melanoma. *Dermatol. Surg.* **28,** 1143–1152

38. Oberley, T. D. (2002) Oxidative damage and cancer. *Am. J. Pathol.* **160,** 403–408

39. Meyskens, F. L., Jr Farmer, P., and Fruehauf, J. P. (2001) Redox regulation in human melanocytes and melanoma. *Pigment Cell Res.* **14,** 148–154

40. Lee, K., W., Lee, H. J., Kang, K. S., and Lee, C. Y. (2002) Preventive effects of vitamin C on carcinogenesis. *Lancet* **359**, 172

41. Koide, T., Kamei, H., Hashimoto, Y., Kojima, T., and Hasegawa, M. (1996) Antitumor effect of hydrolyzed anthocyanin from grape rinds and red rice. *Cancer Biother. Radiopharm.* **11,** 273–277

42. Koide, T., Hashimoto, Y., Kamei, H., Kojima, T., Hasegawa, M., and Terabe, K. (1997) Antitumor effect of anthocyanin fractions extracted from red soybeans and red beans in vitro and in vivo. *Cancer Biother. Radiopharm.* **12,** 277–280

43. Pereda, M. P., Hopfner, U., Pagotto, U., Renner, U., Uhl, E., Arzt, E., Missale, C., and Stalla, G. K. (1999) Retinoic acid stimulates meningioma cell adhesion to the extracellular matrix and inhibits invasion. *Br. J. Cancer* **81,** 381–386

44. Jacob, K., Wach, F., Holzapfel, U., Hein, R., Lengyel, E., Buettner, R., and Bosserhoff, A. K. (1998) In vitro modulation of human melanoma cell invasion and proliferation by all-trans-retinoic acid. *Melanoma Res.* **8,** 211–219

45. Reed, J. A., Finnerty, B., and Albino, A. P. (1999) Divergent cellular differentiation pathways during the invasive stage of cutaneous malignant melanoma progression. *Am. J. Pathol.* **155,** 549–555

46. Fang, D., Hallman, J., Sangha, N., Kute, T. E., Hammarback, J. A., White, W. L., and Setaluri, V. (2001) Expression of microtubule-associated protein 2 in benign and malignant melanocytes implications for differentiation and progression of cutaneous melanoma. *Am. J. Pathol.* **158,** 2107–2115

47. Murphy Ullrich, J. E. (2001) The de-adhesive activity of matricellular proteins: is intermediate cell adhesion an adaptive state? *J. Clin. Invest.* **107,** 785–790

48. Nagao, N., Nakayama, T., Etoh, T., and Saiki, I. M. (2000) Tumor invasion is inhibited by phosphorylated ascorbate via enrichment of intracellular vitamin C and decreasing of oxidative stress. *J. Cancer Res. Clin. Oncol.* **126,** 511–518

49. Buscà, R., Bertolotto, C., Abbe, P., Englaro, W., Ishizaki, T., Narumiya, S., Boquet, P., Ortonne, J. P., and Ballotti, R. (1998) Inhibition of Rho is required for cAMP-induced melanoma cell differentiation. *Mol. Biol. Cell* **9,** 1367–1378

Received April 15, 2004 ; accepted August 5, 2004.

Fig. 1

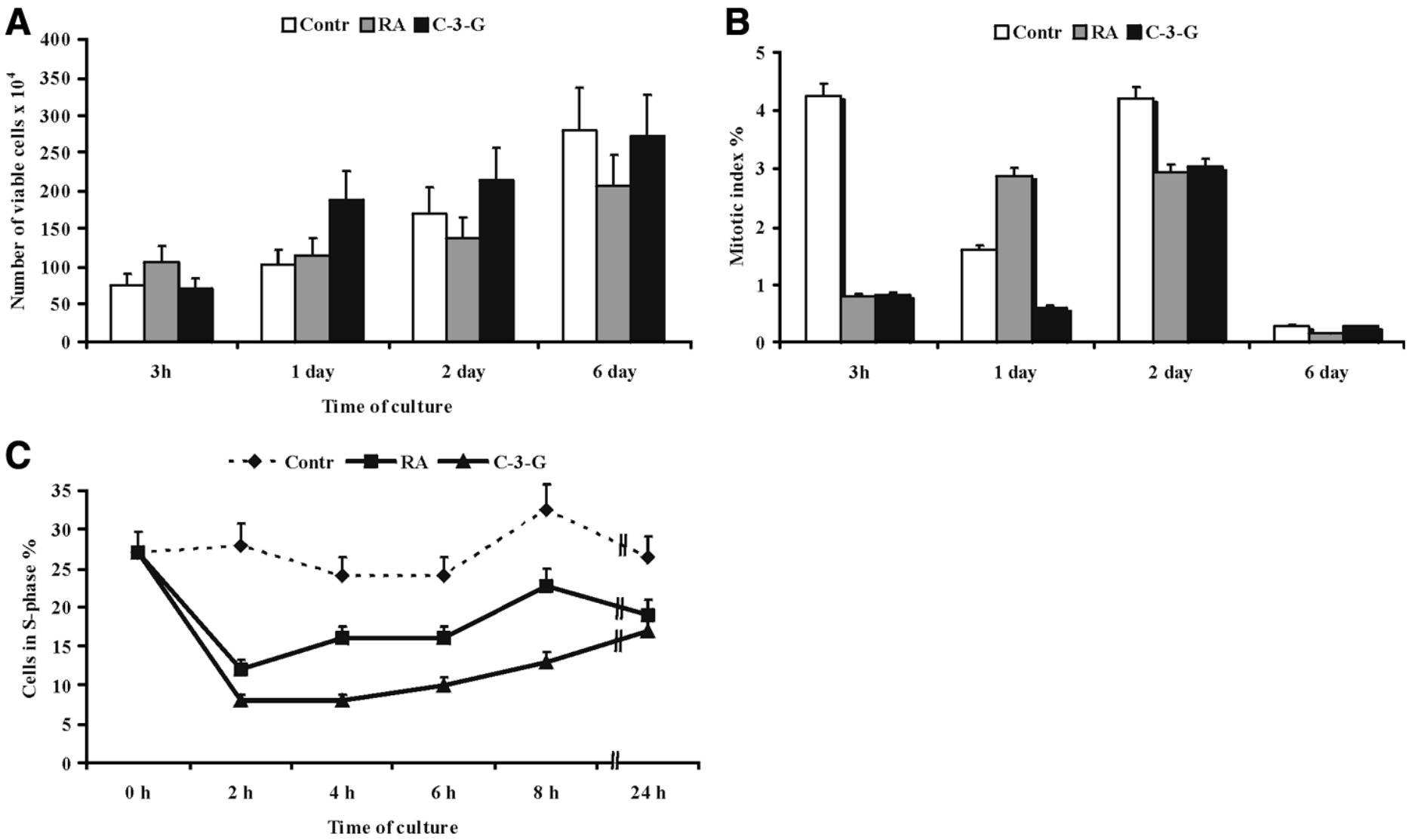

Figure 1. Effect of C-3-G and RA on cell viability (***A***), mitotic index (***B***), and BrdU incorporation (***C***) in TVM-A12 human melanoma cells. ***A*)** Cells were incubated in medium containing less than 0.001% DMSO (control) or the compounds at the concentration of 5 μM. Cells were counted at 3 h, 1, 2, and 6 days of culture and the viability determined by Trypan blue dye exclusion method. ***B*)** the mitotic index was evaluated after 3 h, 1, 2, and 6 days of culture in treated and untreated cells stained with PI; mitotic cells were counted observing at least 1000 cells per sample under confocal fluorescence microscope. ***C*)** BrdU incorporation was measured to determine percentage of cells in S-phase in untreated control (♦) and in 5 μM C-3-G (▲) or RA (■) treated cells, at time ranging from 0 to 24 h of culture. Data are means of 3 different experiments (Student's *t* test $P<0.0001$).

Fig. 2

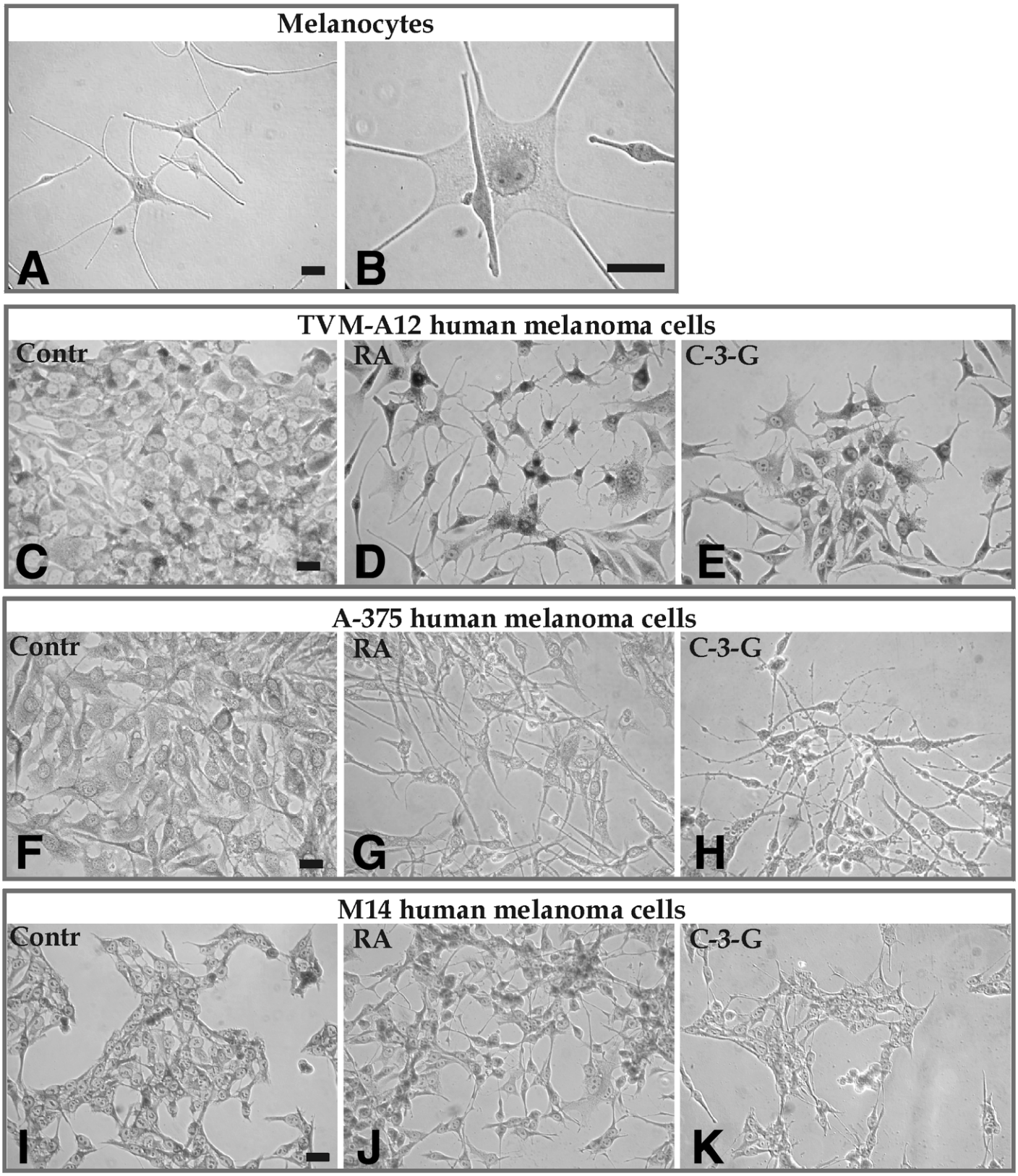

Figure 2. C-3-G treatment induces dendrite outgrowth in human melanoma cells. TVM-A12, A-375 and M14 human melanoma cells were incubated for 5 days with 10 µM C-3-G (***E, H, K***) or RA (***D, G, J***), stained with Wright Giemsa, and observed by phase-contrast microscopy. Both treatment induces, in all melanoma cell line tested, a dramatic dendrite outgrowth, absent in untreated cells (***C, F, I***). ***A, B***) normal melanocytes showing cell dendricity. Bars = 25 µm.

Fig. 3

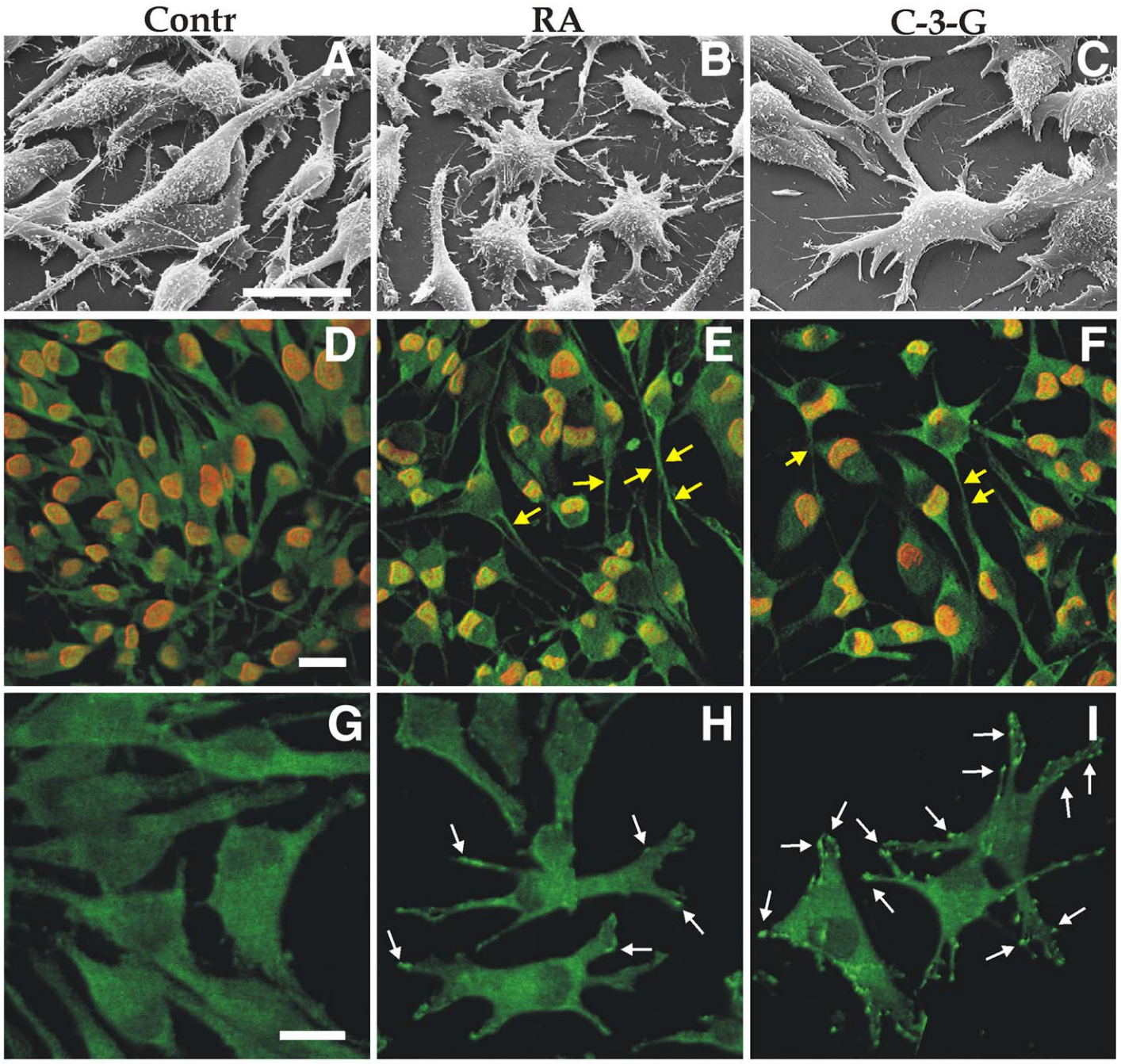

Figure 3. C-3-G treatment induces morphological differentiation, reorganization of microtubular network, and a dramatic increase of focal adhesions in TVM-A12 human melanoma cells. ***A–C***) Scanning electron micrographs of controls (***A***), 5 μM RA (***B***), or 5 μM C-3-G (***C***) treated cells after 5 days of culture. Control cells have spindle shape morphology and tend to grown in superimposed multilayer; both C-3-G and RA treatment induce the formation of long branched dendrites. ***D–F***) Cells were incubated with 5 μM RA (***E***) or C-3-G (***F***) and microtubular network was examined after 5 days of culture by confocal microscopy after immunostaining with rabbit polyclonal antibody raised against chicken tubulin (green hue). Cell nuclei were stained with 2 μg/ml propidium iodide (PI, red hue) in the presence of 0.1 mg/ml RNAase. Yellow arrows point to growing dendrites contained a well-organized microtubular structures. ***G-I***) Distribution of the cytoskeletal component of substratum adhesion plaques vinculin, was examined by confocal microscopy using monoclonal antibody raised against human vinculin after 24 h treatment with 5 μM RA (***H***) or C-3-G (***I***). Compared with untreated control (***G***), an evident increase of focal adhesions (white arrows), was observed in both C-3-G and RA treated cultures. Bars = 25μm.

Fig. 4

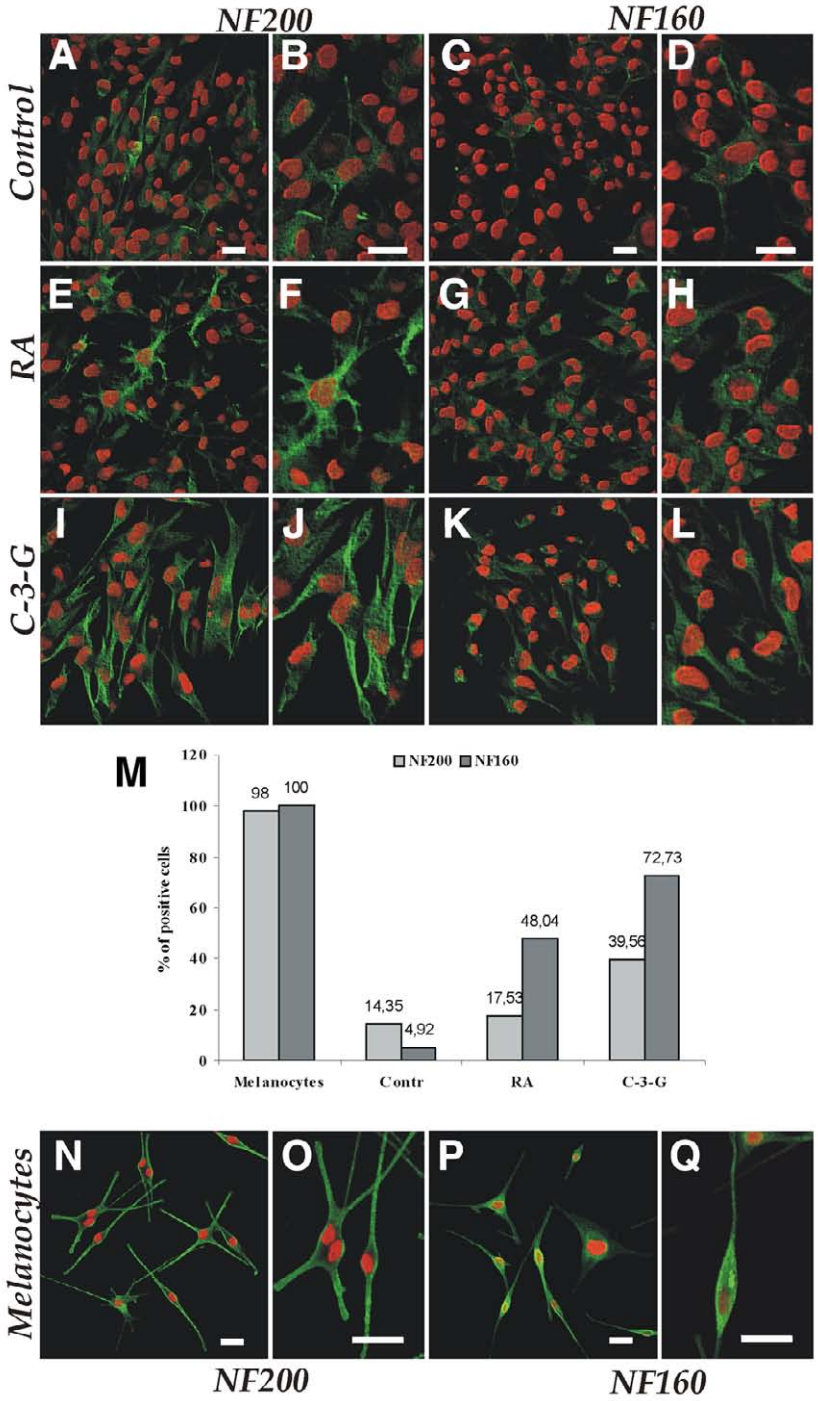

Figure 4. C-3-G treatment induces an increase in expression of NF-160kDa and NF-200kDa and a reorganization of the neurofilament network in TVM-A12 human melanoma cells. ***A–L*****)** TVM-A12 cells were incubated for 5 days with 5 μM C-3-G (***I–L***) or RA (***E–H***) and the intracellular distribution of neurofilament proteins NF-160 kDa and NF-200 kDa, in both treated (***E–L***) and untreated control (***A–D***), was visualized by confocal microscopy after immunostaining using specific monoclonal antibodies. In ***B, F, J, D, H, L***, details at higher magnification of neurofilament network organization (green hue) are reported. Cell nuclei were stained with 2 μg/ml PI (red hue) in the presence of 0.1 mg/ml RNAase. ***M*****)** Expression of neurofilament proteins NF-160 kDa and NF-200 kDa in TVM-A12 cells and melanocytes was evaluated counting the number of positive cells. Percentage of positive cells in treated and untreated control was determined observing at least 500 cells per sample in 3 different experiments. ***N–Q*****)** intracellular distribution of neurofilament proteins NF-160 kDa and NF-200 kDa in primary culture of melanocytes. In ***O*** and ***Q***, details are reported at higher magnification of neurofilament network organization (green hue). Bars = 25 μm.

Fig. 5

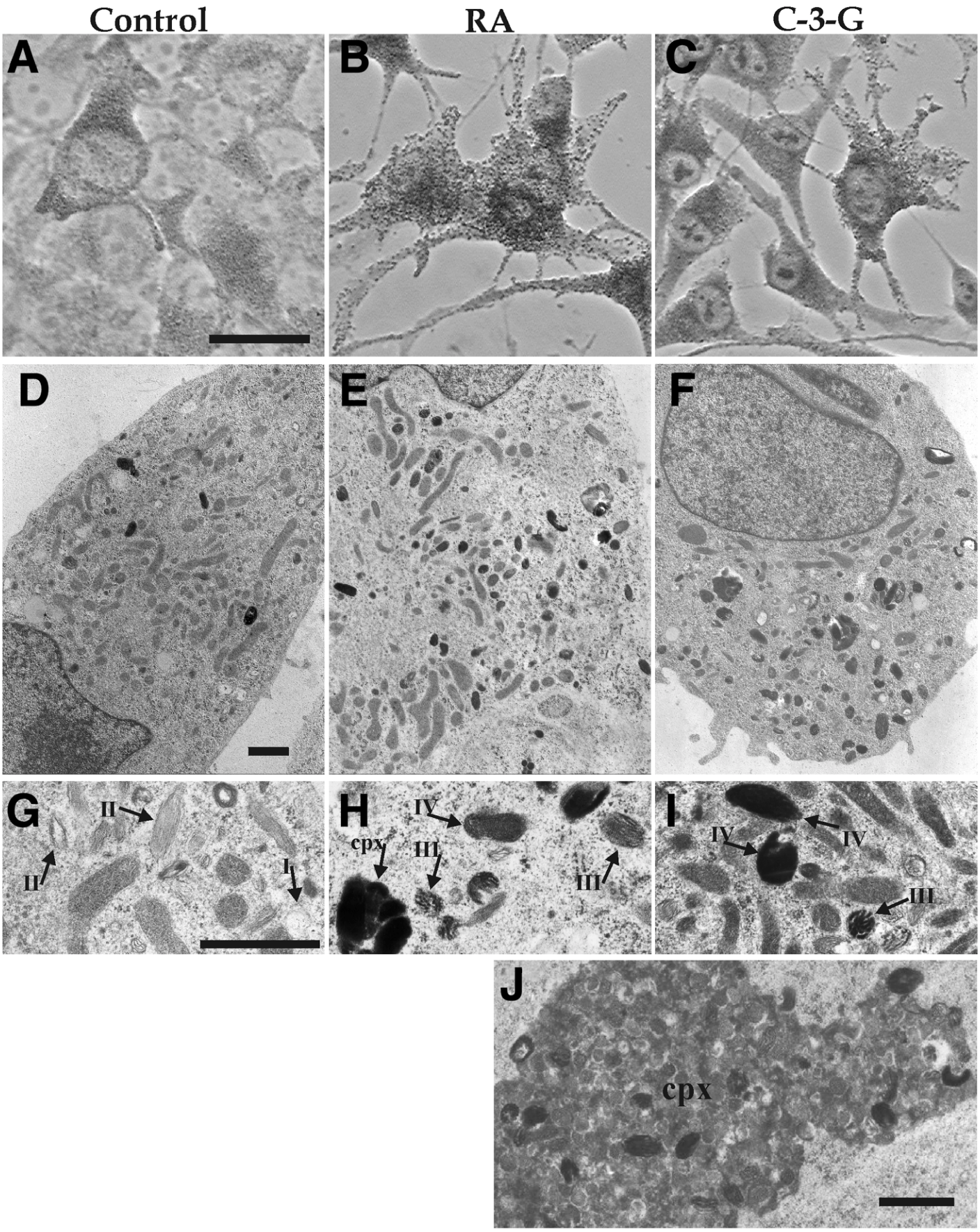

Figure 5. C-3-G treatment induces an increase in melanin synthesis and melanosome maturation in TVM-A12 human melanoma cells. *A-C)* Phase contrast microscopy showing melanin distribution in untreated (***A***) and 10 μM C-3-G (***C***) or RA (***B***) treated TVM-A12 cells after 5 days of culture. Bar = 25 μm. ***D-J)*** Ultrastructural characteristics of TVM-A12 human melanoma cells after treatment with 5μM C-3-G (***F, I, J***) or RA (***E, H***) after 5 days of culture. ***D–F)*** Representative single cell for untreated control (***D***) and C-3-G (***F***) or RA (***E***) treated cultures. ***G–J)*** Details of cytoplasmic space of control (***G***) C-3-G (***I, J***) or RA (***H***). Melanosome stages are indicated by arrows and labeled with Latin number. Note higher size and number of melanosomes in C-3-G or RA treated cells compared with control. In ***J***, a melanosomes complex (*cpx*) in cytoplasm of C-3-G treated cell. Bars = 1 μm.

Fig. 6

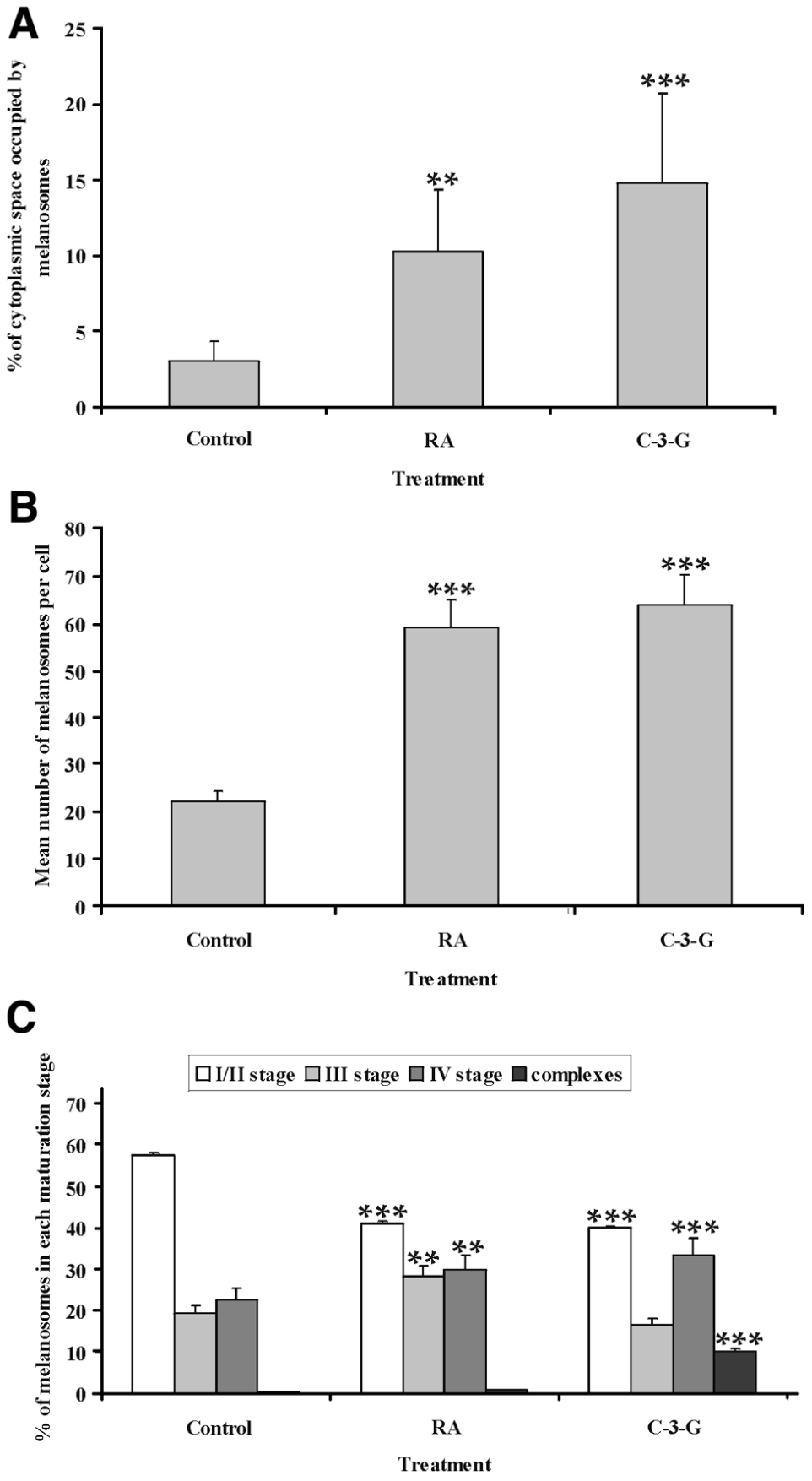
A
% of cytoplasmic space occupied by melanosomes
25
20
15
10
5
0
**
***
Control
RA
C-3-G
Treatment
B
Mean number of melanosomes per cell
80
70
60
50
40
30
20
10
0
***
***
Control
RA
C-3-G
Treatment
C
I/II stage
III stage
IV stage
complexes
% of melanosomes in each maturation stage
70
60
50
40
30
20
10
0
***
**
**
***
***
***
Control
RA
C-3-G
Treatment

Figure 6. Effect of C-3-G and RA treatments on melanosomes area density (***A***) and on number (***B***) and distribution of melanosomes in the different maturation stages (***C***). Data reported in each panel are obtained by quantitative image analysis using the ImageJ processing program and calculated as described in Materials and Methods. ***A*)** Melanosomes area density from control and treated cells is percentage of total cytoplasmic space occupied by melanosomes. ***B*)** Data are mean number of melanosomes per cell. ***C*)** Data are percentage of melanosomes in each maturation stage per cell. (Student's *t* test ****P*<0.001; *****P*<0.0001).

Fig. 7

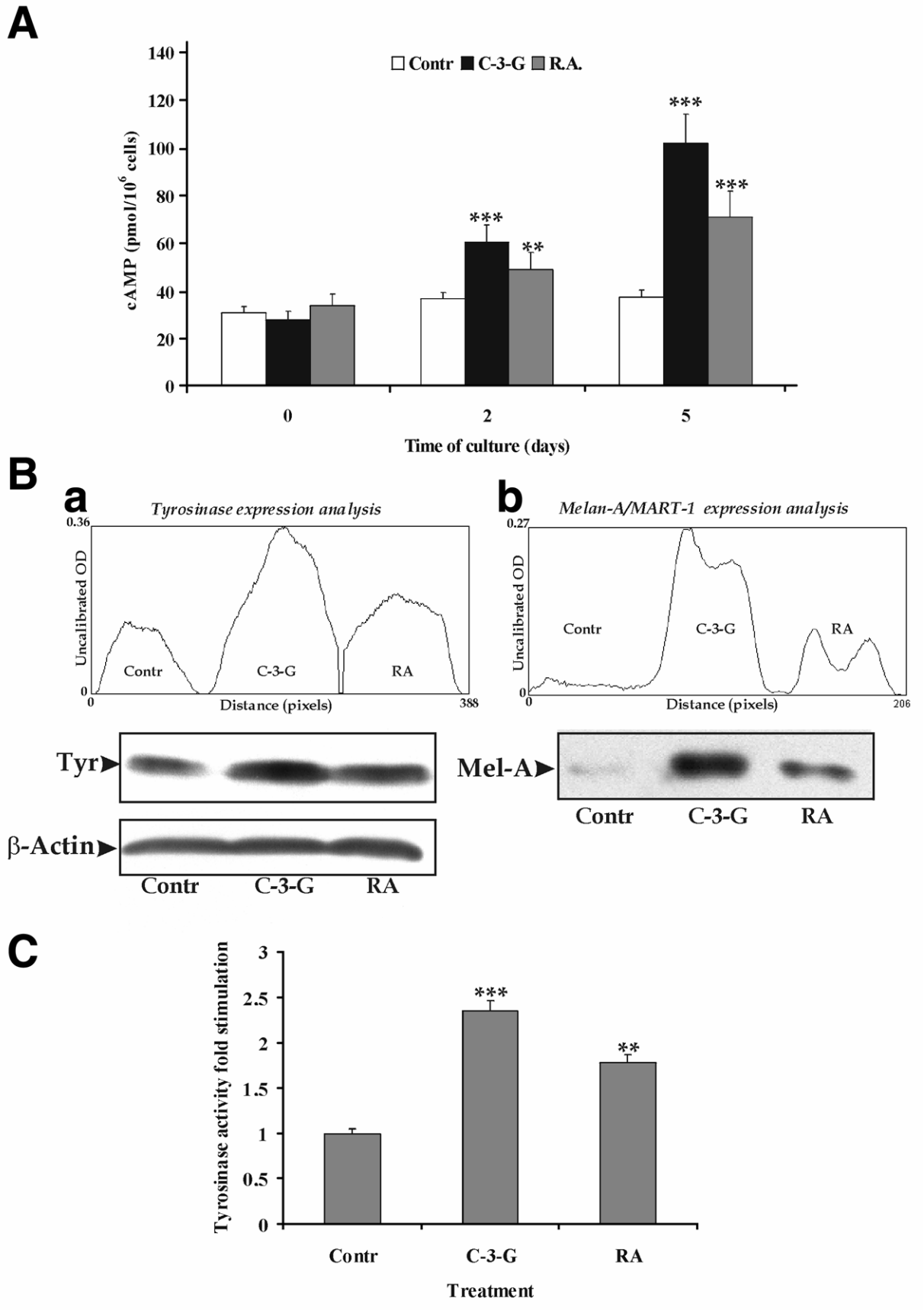
A
Contr
C-3-G
R.A.
cAMP (pmol/10^6 cells)
Time of culture (days)
B
a
Tyrosinase expression analysis
Uncalibrated OD
Distance (pixels)
Contr
C-3-G
RA
b
Melan-A/MART-1 expression analysis
Tyr
β-Actin
Mel-A
C
Tyrosinase activity fold stimulation
Treatment

Figure 7. Effect of C-3-G treatment on cAMP levels, tyrosinase expression and activity and Melan-A/MART-1 expression. *A*) HPLC analysis of the cAMP content in untreated control and 10 μM C-3-G or RA treated cells after 2 and 5 days of culture. Values are expressed as mean and are representative of 3 experiments. ***B*)** 40γ of solubilized proteins from untreated control and cells treated for 5 days with 10 μM C-3-G or RA were subjected to Western blot analysis using mouse monoclonal anti-tyrosine hydroxylase for detection of tyrosinase (***Ba***) or Melan-A/MART-1 antigen (***Bb***). Blot was simultaneously incubated with anti-β-actin antibody to show that each electrophoretic lane was loaded with the same amount of protein. ***Upper panels*)** Levels of tyrosinase or Melan-A/MART-1 antigen expression were quantified by quantitative image analysis using the ImageJ processing program and expressed as uncalibrated Optical Density (OD). ***C*)** Tyrosinase activity in untreated control and 10 μM C-3-G or RA treated cells after 2 days of culture, estimated by measuring the rate of oxidation of L-DOPA as described in Materials and Methods. Obtained activity was corrected by amount of protein for each experimental condition and reported as fold stimulation with respect to control. Data are representative of 3 experiments performed in triplicate. (Student's *t* test $^{**}P<0.001$; $^{***}P<0.0001$).